Available online at www.sciencedirect.com
ScienceDirect
Journal of Marine Systems 71 (2008) 149–158
JOURNAL OF MARINE SYSTEMS
www.elsevier.com/locate/jmarsys

Connectivity in the northern Gulf of California from particle tracking in a three-dimensional numerical model

S.G. Marinone [a,*], M.J. Ulloa [b], A. Parés-Sierra [a], M.F. Lavín [a], R. Cudney-Bueno [c]

[a] *Department of Physical Oceanography, CICESE, Ensenada, Baja California, Mexico*
[b] *Department of Physics, University of Guadalajara, Guadalajara, Jalisco, Mexico*
[c] *Department of Natural Resources, University of Arizona, Tucson, Arizona, USA*

Received 4 March 2006; received in revised form 28 April 2007; accepted 20 June 2007
Available online 10 July 2007

Abstract

The northern Gulf of California, Mexico, is one of the most productive and diverse marine ecosystems in the world. It currently harbors three marine protected areas, including two biosphere reserves. Despite its significance as a conservation site and its importance for Mexico's fisheries, proper knowledge of population connectivity and larvae dispersal from spawning sites is largely lacking. Our study focuses on connectivity in the northern gulf resulting from advection by currents and turbulent diffusion during summer, the main spawning period of various key commercial species. We calculated connectivity matrices in the northern Gulf from currents produced by the output of a three-dimensional baroclinic numerical model and a random walk process to simulate turbulent motions. We released 2000 hypothetical passive particles in each of 21 areas along the coast (between 0–60 m deep) during the summer and followed their trajectories for periods of 2, 4, 6, and 8 weeks. For the case of full time transport, the effects of tidal currents are minimal in the overall dispersal of passive particles on the time scales studied. However, this can be substantially altered if the particles are allowed to avoid being transported for periods of time; this is illustrated by striking differences between the connectivity matrices obtained by modeling also night-only and day-only advection. This "order zero" connectivity study (i.e., not including realistic larvae behavior, which is species-specific) reveals that during the summer spawning season of key commercial species, regional hydrodynamics produce a cyclonic downstream connectivity along the coast, from the mainland to the Baja California coast. Our results provide the basis for a full connectivity study where larvae behavior and settlement habitat will be included.

Keywords: Connectivity; Gulf of California; Fisheries; Lagrangian circulation

1. Introduction

The northern Gulf of California (NGC, Fig. 1) is a chief supplier of Mexican fisheries and is considered a conservation priority area both in Mexico as well as internationally (Carvajal et al., 2004), harboring 3 marine protected areas, including 2 biosphere reserves. Despite its importance, knowledge about larvae dispersal and population connectivity is largely lacking, even though these are key factors for the development of proper fisheries management guidelines, including reserve design (Largier, 2003).

Worldwide there is much uncertainty regarding larval biology and behavior (James et al., 2002). In the NGC, species' population dynamics, particularly in regards to movement and dispersal in their early life histories, is

* Corresponding author. PO BOX 434844, San Diego, Ca., 92143-4844, USA.
E-mail address: marinone@cicese.mx (S.G. Marinone).

0924-7963/$ - see front matter © 2007 Elsevier B.V. All rights reserved.
doi:10.1016/j.jmarsys.2007.06.005

poorly known. For example, during summer Aragón-Noriega and Calderón-Aguilera (2001) consistently found 22 days-old shrimp postlarvae off the peninsula coast and 28 days old off the mainland. This is very puzzling and still unexplained since the circulation at this time of year is cyclonic and the reproductive areas have mainly been reported close to the mainland coast.

Dispersal patterns of marine organisms are species-specific and dependent on behavior and hydrodynamics. It is known that fish larvae follow ambient cues to successfully reach nursery areas or survive (e.g. Wolanski et al., 1997; Armsworth, 2001; Bradbury and Snelgrove, 2001; Hofmann et al., 2004). Ultimately, net displacement is largely the result of regional hydrodynamics and the species' motility throughout its life history. However, locomotion is limited during the early larvae stages of various organisms, and many of these (particularly mollusks) have very limited or null active movement during their adult stages. For these species, displacement can be assumed passive, hydrodynamics being the main factors controlling their dispersal. These organisms will permeate into large landscapes, while those with active behavior could be more geographically constrained (Armsworth and Roughgarden, 2005), depending on their specific behavior.

As a first step in studying connectivity patterns in the NGC, in this article we calculate connectivity matrices along the coastal area of the NGC (between 0 and 60 m depth) during the summer months, when various important commercial species spawn. We track sets of particles for up to two months which, excluding a limited number of species, is considered to be a maximum time length for larvae to remain in the water column (Bernardi and Lape, 2005). The field of currents used to conduct particle tracking is obtained from a 3D baroclinic numerical model (Marinone, 2003). The temporal scales resolved by the model (due to forcing) are tidal and seasonal.

During summer, the general surface Lagrangian circulation in the NGC consists roughly of a basin-size cyclonic gyre (Lavín et al., 1997; Carrillo-Bribiezca et al., 2002), which lasts from about June to September. The gyre is caused by annual-period forcing by the monsoonal winds, the Pacific Ocean, and the heat flux through the surface (Beier and Ripa, 1999). This circulation has been modeled numerically, from an Eulerian perspective, by Beier (1997) and Palacios-Hernández et al. (2002) with a two-layer model and by Carbajal (1993) and Marinone (2003) with full three-dimensional (3D) models. Gutiérrez et al. (2004) determined the Lagrangian circulation from the output of Marinone (2003) using only the upper-layer model currents without vertical excursion of the particles, and obtained results in agreement with the surface drifter observations of Lavín et al. (1997). Marinone (2006) calculated the full 3D Lagrangian circulation of the northern gulf with satisfactory results compared again with Lavín et al. (1997). In addition, Marinone and Lavín (2005) compared the harmonic constants of the model with current meter observations and obtained also good agreement. In essence, the numerical model developed by Marinone (2003) produces "realistic" currents on seasonal and tidal scales. To date, this 3D model provides the best available synoptic current field of the gulf and therefore we rely on it to calculate the connectivity matrices in this study.

However, it is important to stress that the approach we have taken, which is based on pure hydrodynamics, should be considered as the "order zero" interaction between larval dispersal and hydrodynamics (i.e., that due to advection and diffusion), and thought of as the "basic" or "background" connectivity in the area. Strictly speaking, it provides an understanding of connectivity of nutrients, pollutants, and of larvae that are passive or have limited locomotion. A similar work for the Australian continent has been conducted by Condie et al. (2005) in which they estimate the probability, by means of a web-tool, that two regions are connected.

2. Numerical model and particle tracking

We released 2000 particles in each one of 21 equal-area regions shown in Fig. 1, tracking each particle for up to two months (the maximum expected length of the larvae of key species) during the summer (the main spawning season). Some of these areas comprise key reproductive/spawning sites of various important commercial species such as groupers (*Mycteroperca* spp), snapper (*Hoplopagrus guentherii*), black murex snail (*Hexaplex nigritus*), rock scallop (*Spondylus calcifer*) and blue shrimp (*Litopenaeus stylirostris*) (Richard Cudney-Bueno, unpublished data). While for some species of the region spawning sites are still unknown and are probably in deep water, for many commercial species of interest we know that spawning occurs in shallow water (0–20 m) or that they have a pelagic larval life in depths up to 60 m (Bernardi and Lape, 2005). It is therefore reasonable to choose as the initial area of release the area between the shore and the 60 m isobath and from the surface to the bottom. We chose to use 2000 particles after having run the model with larger numbers of particles and finding that the connectivity matrices were very similar.

The velocity field used to calculate the particle trajectories came from the Gulf of California implementation of the three-dimensional baroclinic Hamburg

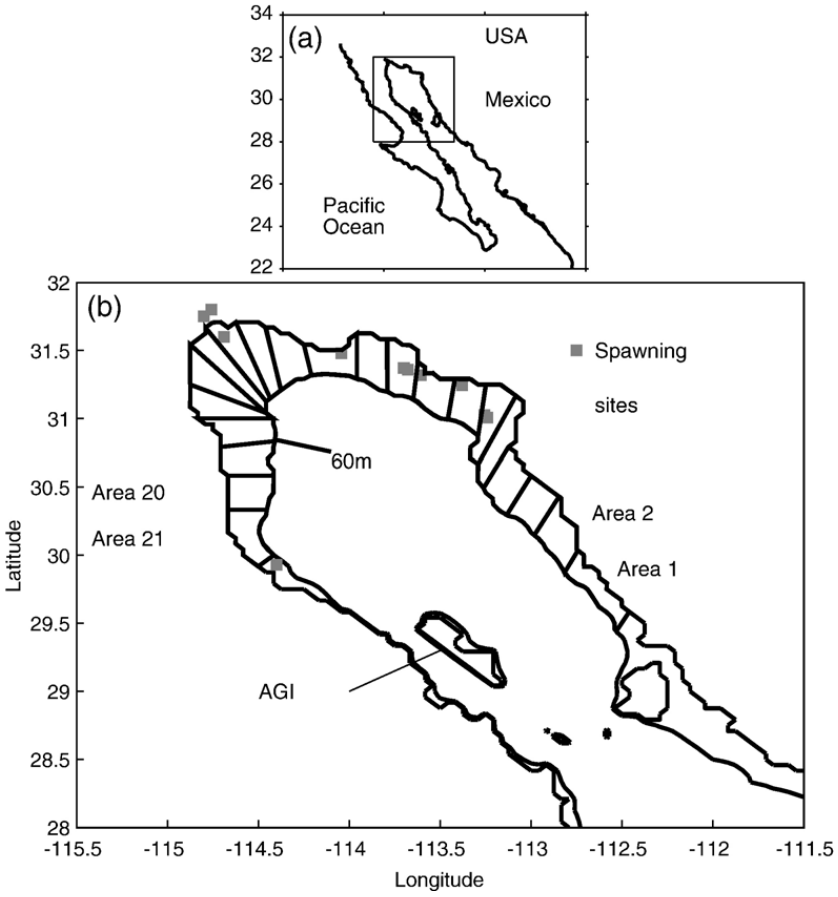

Fig. 1. (a) Study area (rectangle) in the Gulf of California, and (b) location of the different areas were particles are seeded. There are 21 areas (between the coastline and the 60 m depth isobath), numbered anticlockwise (only few are labeled), and all have approximately the same surface area. The gray squares mark the position of spawning points of some fisheries during summer. AGI stands for Angel de la Guarda Island.

Shelf Ocean Model (HAMSOM) developed by Backhaus (1985). The model is described in detail for the Gulf of California by Marinone (2003) and Mateos et al. (2006), and in general references therein. Its domain has a mesh size of $2.5' \times 2.5'$ ($\sim 3.9 \times 4.6$ km) in the horizontal and 12 layers in the vertical with nominal lower levels at 10, 20, 30, 60, 100, 150, 200, 250, 350, 600, 1000 and 4000 m. The model equations are solved semi-implicitly with fully prognostic temperature and salinity fields, thus allowing time-dependent baroclinic motions.

The horizontal resolution used means that some of the important and complex coastal environment is not resolved, as much higher resolution is needed for the bathymetry and the coastline. However, it is the aim of the overall project to reach the required resolution for specific areas through the use of nested models with appropriate bathymetry.

The model is started from rest, and the time step is 300 s. It is forced with tides, climatological winds, climatological hydrography at the mouth of the gulf, and climatological heat and fresh water fluxes at the air-sea interface. It becomes periodically stable after three years and the results for this study were obtained from the fourth year of the model. As shown by Marinone (2003), the model adequately reproduces the main seasonal signals of surface temperature, heat balance, tidal elevation and surface circulation in the NGC as reported by Lavín et al. (1997).

The use of climatological wind forcing is justified during the summer because the main wind signal is seasonal. From the authors' experience, synoptic effects does not seem to affect the circulation at the scales studied here, and there are no storms in summer, except when hurricanes enter the Gulf, which occur rarely and affect mostly the southern part of the Gulf.

Particle trajectories were calculated following the advection/diffusion scheme described in Visser (1997) and Proehl et al. (2005). The Lagrangian trajectories are due to the Eulerian velocity field plus a random-walk contribution related to turbulent eddy diffusion processes. The values of the diffusivities are taken from the numerical model, and since the vertical diffusivity is not constant, a pseudo-advective term is introduced to prevent

particles from walking away from areas of high to low diffusivities. Therefore, the position of the particles are calculated as,

$$X(t+\delta t) = X(t) + X_a(t) + R_x \sqrt{(2A_h \delta t/\sigma_x^2)}, \quad (1)$$

$$Y(t+\delta t) = Y(t) + Y_a(t) + R_y \sqrt{\left(2A_h \delta t/\sigma_y^2\right)}, \quad (2)$$

$$Z(t+\delta t) = Z(t) + Z_a(t) + R_z \sqrt{\left(2A_v \delta t/\sigma_z^2\right)} + \delta t \partial A_v/\partial Z, \quad (3)$$

where (X, Y, Z) are the particle positions in the zonal, meridional, and vertical directions, respectively, at time t. X_a, Y_a, and Z_a are the advective displacements obtained by integrating the velocity field, $V_a=(u, v, w)$. The velocity at each particle position is calculated by bilinear interpolation of the instantaneous Eulerian velocity fields from the numerical model which were saved every hour. R_x, R_y, and R_z are random variables with zero mean and variance σ_x^2, σ_y^2, and σ_z^2, respectively. For uniform distribution between -1 and 1 the variances are 1/3 (Visser, 1997). A_h and A_v are the horizontal and vertical diffusivities, respectively, and are taken from the Eulerian numerical model. Eqs. (1) and (2) differ from (3) in one term, the last in (3), which takes into account the time and spatial variability of A_v. The horizontal eddy diffusivity is constant ($A_h=100$ m^2 s^{-1}) and therefore the corresponding terms do not contribute to the particle displacements. We explored the sensitivity of the model results to the choice of A_h, and found that it is necessary to increase it by one order of magnitude to obtain important upstream connectivity. However, for the vertical, $A_v=A_v(x,y,z,t)$ the gradient is calculated and interpolated for the individual particle positions at each time step. In the numerical model A_v is calculated following Kochergin (1987), as $\alpha|\partial/z\ v|/(1+\beta R_i)$, where R_i is the Richardson number, $\alpha=10$ m^2 and $\beta=10$. The values of A_v vary from 0 to ~0.03 m^2 s^{-1}, with a temporal and spatial average of 0.013 m^2 s^{-1} and a standard deviation one order of magnitude smaller.

3. Results and discussion

Fig. 2 shows the first model layer (0–10 m), time-averaged currents for the two-month period of simulation. Below this surface layer the currents are very similar, although there is some vertical shear, especially in the deeper parts. The cyclonic flow clearly dominates the circulation, there are strong horizontal shears, and the maximum speeds are in the range 10–15 cm s^{-1}.

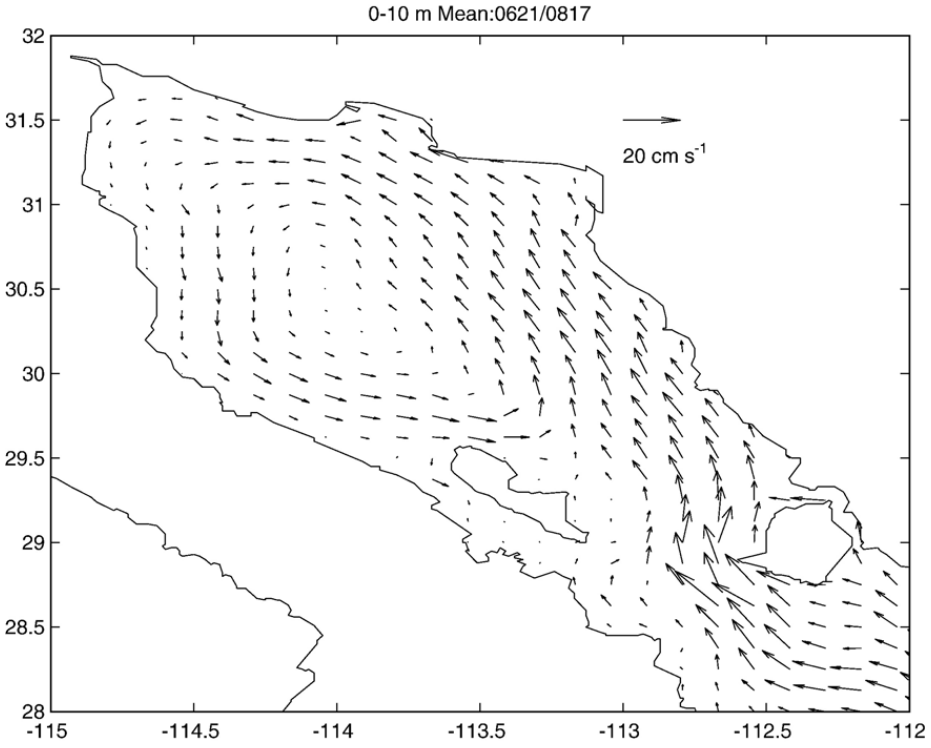

Fig. 2. Time-averaged currents for the first model layer (0–10 m). The period of averaging is from June 21 to August 17. Only one in every three arrows is plotted for clarity.

This cyclonic circulation has a seasonal time scale (reversing to anticyclonic during winter) but during the time period of interest the currents are basically as shown in Fig. 2. This current field is responsible for the dispersal of nutrients, pollutants and passive larvae in general.

The instantaneous currents are faster than the low frequency currents, since they include tidal currents. Fig. 3 shows the evolution of the surface current field during half a tidal cycle: during flood the flow is up-gulf everywhere, while during ebb it is down-gulf. However, although the instantaneous flow does reverse within the tidal cycle, in time scales of a few days the low-frequency, or residual flow (Fig. 2), dominates the trajectory of the (non active) particles (Marinone, 2006).

Fig. 4 shows the position of the particles after 2, 4, 6, and 8 weeks of continuous advection/diffusion. These distributions are in accordance with the consistent finding of high densities of juvenile rock scallops (*Spondylus calcifer*) and black murex (*Hexaplex nigritus*) found to the north of key spawning sites (Cudney-Bueno, 2007), species whose larvae can be considered passive. Essentially the cloud of particles travels counterclockwise, which was anticipated given the currents shown in Figs. 2 and 3. As they travel, the clouds of particles stretch and spread out, and although many particles remain within the 0 to 60 m isobaths, most escape to deeper areas. By the end of the two-month tracking period (Fig. 4d) even particles from area 1 have reached area 21 (in the peninsular side). While some of the particles released on the peninsula side are found around Angel de la Guarda Island, others seem to have returned to the north, following the eastern branch of the cyclonic gyre. Particles released in the Baja California coast never reach the continental coast during the tracking period.

Fig. 5 shows the corresponding connectivity matrices C_{ij} (t) for $t=2$, 4, 6, and 8 weeks after release, as percentage of the 2000 seeded particles (in each region). The vertical axis (j) represents the areas of release and the horizontal axis (i) represents the areas where the particles are found at the end of the time period. Thus C_{ij} represents the concentration of particles found in area i that came from area j, at the specified time after release. Therefore row j of the connectivity matrix gives the number (percentage) of particles released in that area (j) that were found in every one of the other areas ($i=1$–21), after the elapsed time t. Column i gives the percentage of particles found in that area (i) that came from each one of the release areas ($j=1$–21), after an elapsed time.

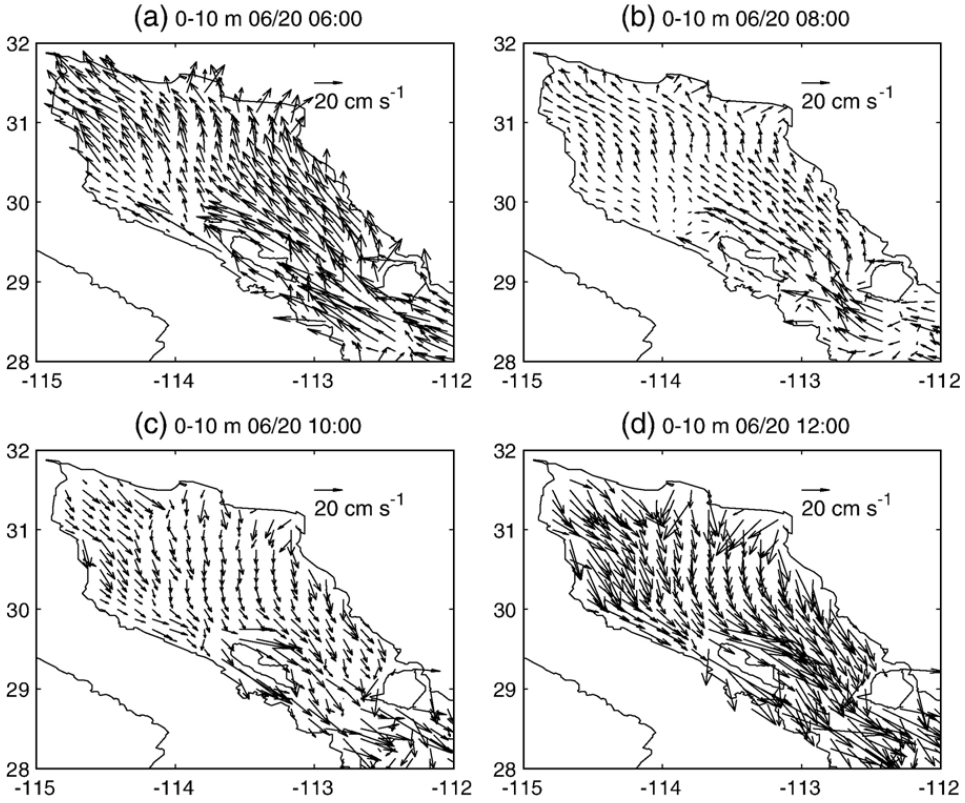

Fig. 3. Instantaneous currents for the first model layer (0–10 m) for June 20. Flood corresponds to hour (a) 6:00 and (b) 08:00 and ebb is occurring during hours (c) 10:00 and (d) 12:00. Only one in every three arrows is plotted for clarity.

If there were no currents but only diffusion, the matrices would show a bell shape with maxima in the main diagonal, which would spread outward with time. However, as time passes, the area of higher percentage moves to the high-numbered areas, which represents a net counterclockwise displacement of the particles (Fig. 5). The distance between area 1 and 21 (along the coastline) is ~450 km, and the mean distance traveled by the particles from one area to their final destination in 8 weeks is ~300 km.

We repeated all the experiments starting at different phases of the tide, and during spring and neap tides, and found no significant difference with the results just shown. This means, as suggested before, that in the time scales under study, tidal currents are of limited importance for non-active particles, and that the residual currents determine connectivity. Tidal currents only make the trajectories to oscillate, with loops the size of the tidal excursion (~5–8 km) stretched along the general path of the residual currents. However, for larvae that have active motile behavior, such as the ability to select favorable currents by changing their position in the water column, tidal currents would likely be very important indeed (see Hogan and Mora, 2005). Likewise, given the intense tidal flows of the NGC, for species with short-lived larvae stages, tidal currents, the timing of spawning and the species-specific larval behavior could become determinant; however, the study of such short-time scales is beyond the focus of this article.

An illustration of the importance of motility was obtained with our model by restricting the transport of the particles to only day or only night. Fig. 6 shows the connectivity diagrams after 4 and 8 weeks corresponding to those of Fig. 5: they are strikingly different. The connectivity is strongest (meaning that more particles are present) for the case of day-time advection (Fig. 6), followed by the full-time-advection case (Fig. 5), while when they are transported during the night the weakest connectivity is obtained (Fig. 6). This is the result of the combination of the selective transport during the 12 h of day or night with the different periods of all the tidal components, of which only S2 coincides exactly with the selected period of allowed transport. The consequence of the S2 locking of the diel vertical migration on horizontal dispersion was discussed by Hill (1994) who found that the phase modulates the direction of the migration-induced transport. In our case, which includes many component ellipses, it seems that the orientation of the ellipses relative to the residual current may also be relevant.

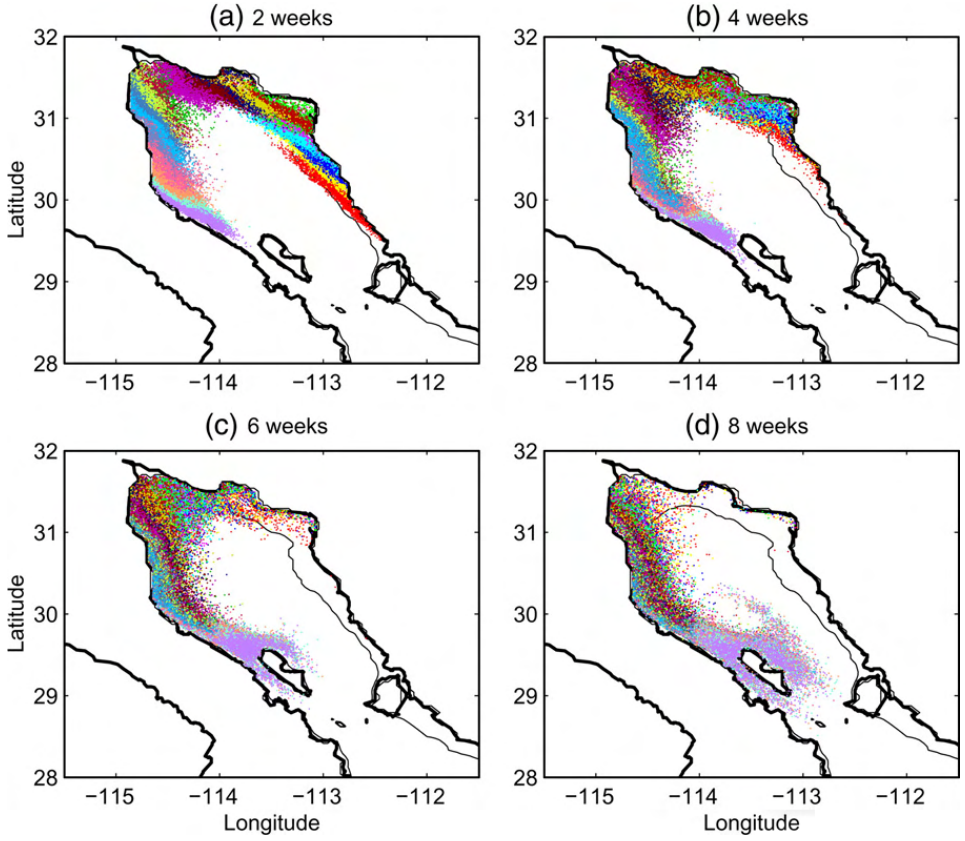

Fig. 4. Final position of the particles after (a) 2, (b) 4, (c) 6, and (d) 8 weeks. Their initial positions (21 positions areas) are shown in Fig. 1b. The 60 m isobath is shown.

The distributions of particles corresponding to the dispersion diagrams with advection only during the day or only during the night are shown in Fig. 7. For the night-only case (Fig. 7, left panels), the areas 6 to 17 are almost empty because the particles have moved offshore. In the day-only case, the particles remain mostly inside the 0–60 m coastal zone. The principal diurnal and semidiurnal tidal ellipses (Marinone and Lavín, 2005) are almost normal to the isobaths (and to the residual current) for areas 6 to 17. In the sampled time period, the diurnal inequality was such that the tidal currents during the night were weaker than during the day, which may influence the results of this particular exercise. This example illustrates the importance of the vertical migration pattern upon connectivity, although of course larvae behavior is species-specific and not restricted to diel vertical migration and attachment to the bottom.

The connectivity pattern found in this study is a very robust result. The dynamics of the circulation of the Gulf of California are well understood and supported by data (see, e.g., review by Lavín and Marinone, 2003), and as a consequence the numerical models (even with a relatively rough resolution) reproduce a very large proportion of the current variability, most of which is seasonal and tidal. This is a very positive situation for connectivity studies. Although including larvae behavior in numerical models is relatively straightforward, the knowledge about larvae behavior is quite limited. More future effort should be devoted to understanding larvae behavior of key commercial species.

Our study is part of an interdisciplinary project (www.pangas.arizona.edu) which will involve a characterization of small-scale fisheries in the NGC in terms of population connectivity, key habitat of targeted species, reproductive sites/times of targeted species, spatial-temporal distribution of fishing activities, and linkages between regional bio-physical and social processes. As part of the broader study, life histories of key species are being constructed from the literature and from specific studies; once obtained, appropriate

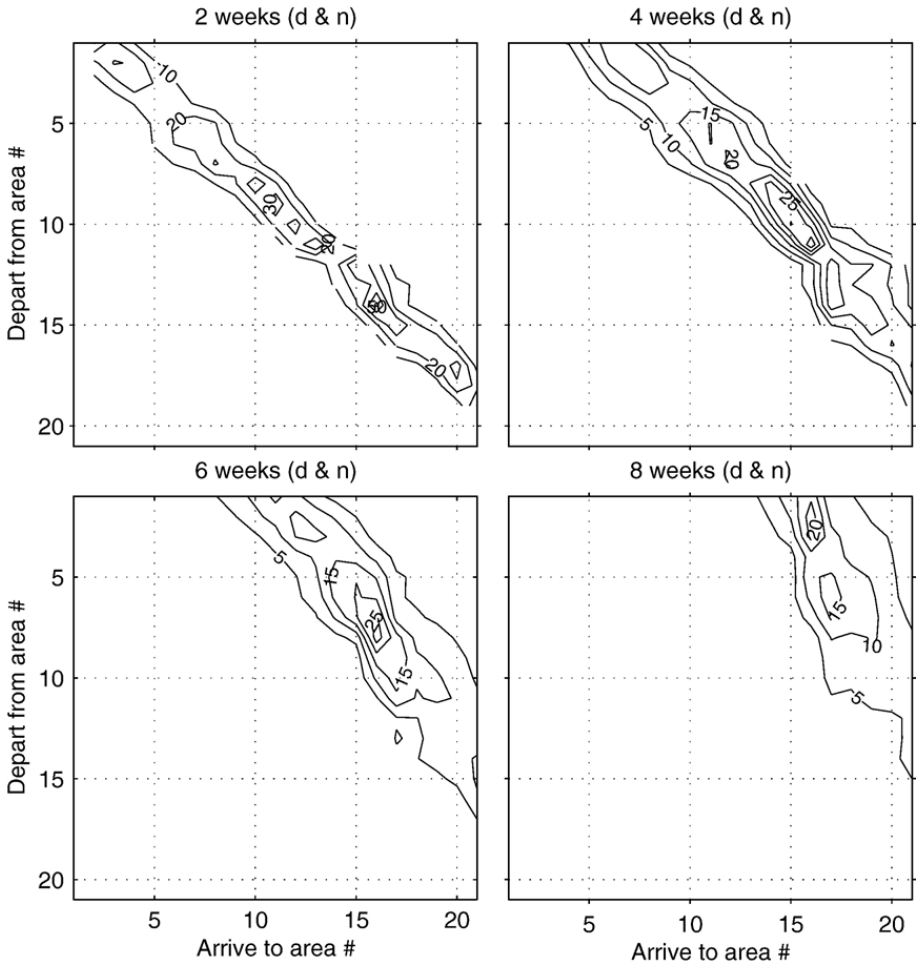

Fig. 5. Connectivity maps in (in percentage) after 2, 4, 6, and 8 weeks periods. The total number of particles seeded in each area is 2000 (a total of 21 × 2000). The axes represent the area numbers given in Fig. 1: the vertical axes represent release areas, and the horizontal axes represent particle arrival areas.

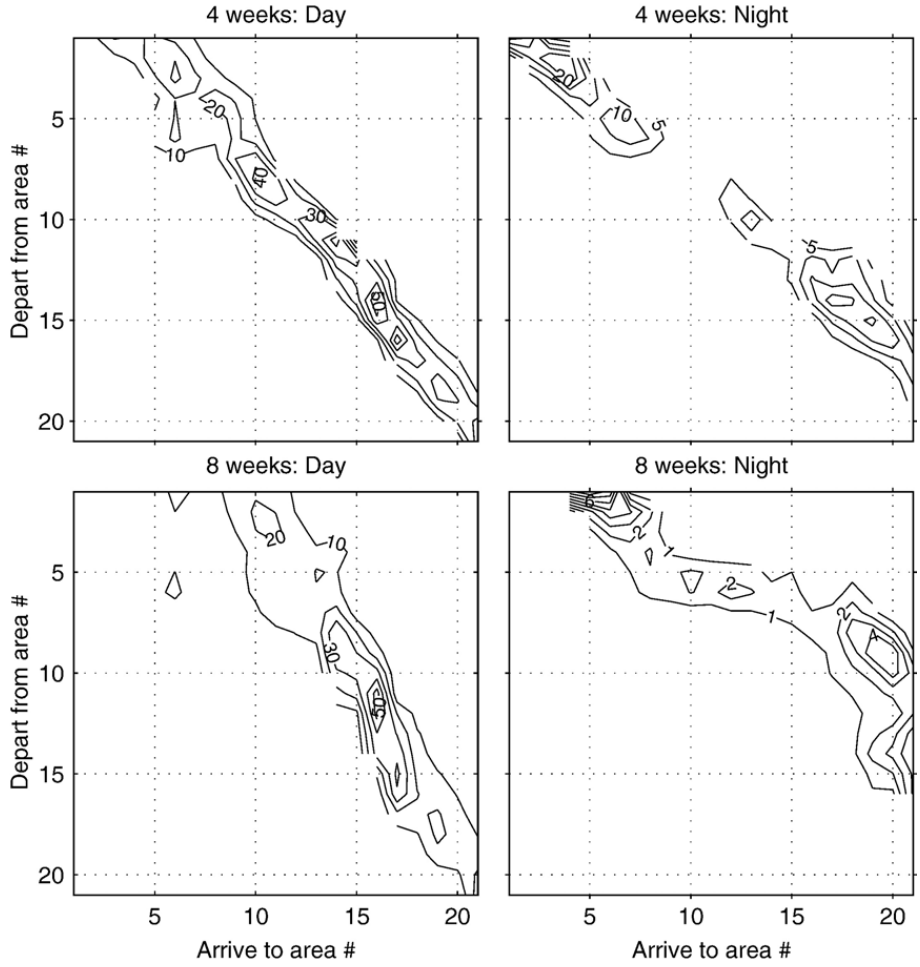

Fig. 6. Connectivity maps in (in percentage) after 4 and 8 weeks periods. The left and right frames correspond to particles transported during day and during the night only, respectively. The total number of particles seeded in each area is 2000 (a total of 21 × 2000). The axes represent the area numbers given in Fig. 1: the vertical axes represent release areas, and the horizontal axes represent particle arrival areas.

biological and ecological information (i.e. key breeding aggregation and spawning sites, spawning times, larvae settlement habitat, larvae behavior) will be incorporated into our model to assist the design of management strategies for small-scale fisheries in the region.

4. Conclusion

We calculated connectivity matrices in the NGC from currents produced by a three-dimensional baroclinic numerical model and a random walk process to simulate turbulent motions. The period of study is for summer, when a basin-wide cyclonic gyre is well established. Particles were released at 21 equal-area regions along the coast. For the period (summer) and time interval (two months) studied there is high cyclonic (anti-clockwise) connectivity and basically null connectivity in the opposite direction. The particles' main trajectory follows the large-scale circulation and is dominated by residual flows, with tides only making particles oscillate along the trajectory. However, for larvae capable of selecting favorable currents by changing their position in the water column, tidal currents will likely be of high importance. In addition, given the intensity of tidal currents in the NGC, for those species whose larvae are competent to settle soon (few days) after being released (e. g. some lecithotrophic larvae), tidal currents could be determinant.

This study provides a basis to begin comprehending connectivity of fisheries in the NGC and to allow the development of more complex models. Since the horizontal resolution is still somewhat large for detailed local connectivity studies, in the future we will use a finer mesh and will incorporate species-specific larvae behavior and distribution of key settlement habitats. In addition, results obtained through models will be ground-tested with data on population genetics and species-specific trace elements. Ultimately, the efforts begun through this

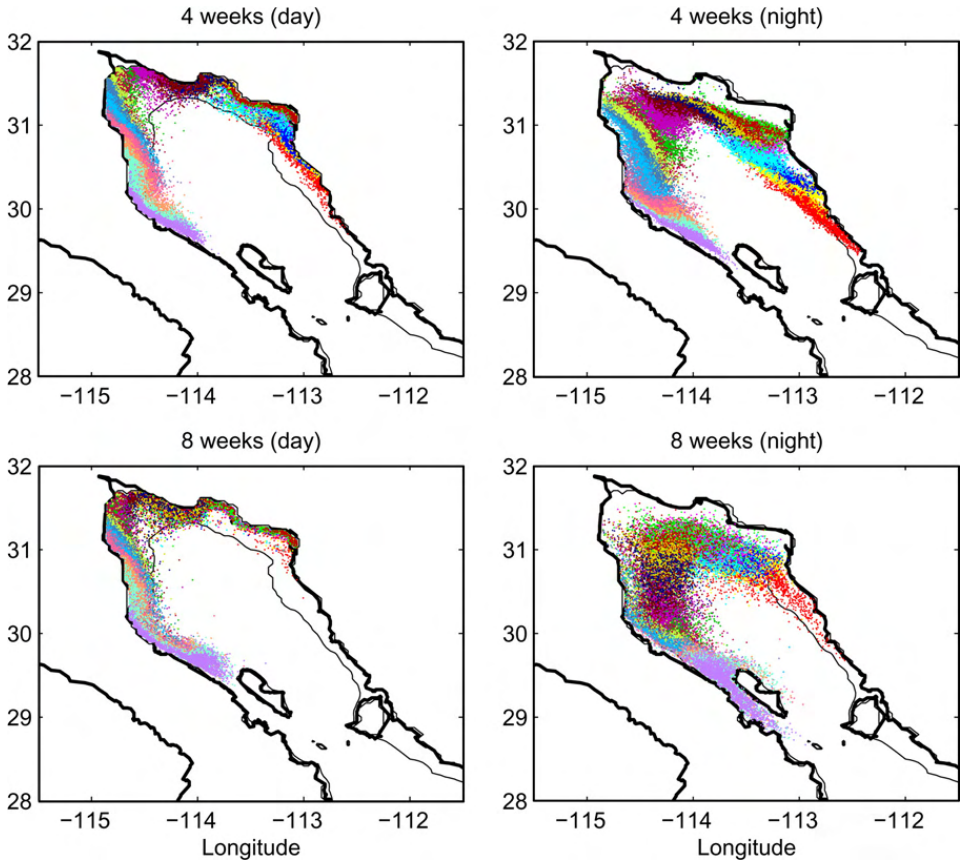

Fig. 7. Final position of the particles after 4 and 8 weeks. The left and right frames correspond to particles transported during day and during the night only, respectively. The 60 m isobath is shown.

study will help direct policy towards a better-informed and effective management of one of the region's most influential and impacting economic activities.

Acknowledgements

This research forms part of the interdisciplinary PANGAS project. Funding was provided by the David and Lucile Packard Foundation (grant # 2004-27789), by the Consejo Nacional de Ciencia y Tecnología (CONACyT) through grants 44055 and D41881-F, and by CICESE's regular operational budget. MFL was as on sabbatical leave at SIO/UCSD thanks to a UCMEXUS-CONACyT grant.

References

Aragón-Noriega, E.A., Calderón-Aguilera, L.E., 2001. Age and growth of shrimp postlarvae in the Upper Gulf of California. Aquatic Journal of Ichthyology Aquatic Biology 4 (3), 99–104.

Armsworth, P.R., 2001. Directed motion in the ea: efficient swimming by reef fish larvae. Journal of Theoretical Biology 210, 81–91. doi:10.1006/jtbi.2001.2299.

Armsworth, P.R., Roughgarden, J.E., 2005. The impact of directed versus random movement on population dynamics and biodiversity patterns. The American Naturalist 165, 449–465.

Backhaus, J.O., 1985. A three-dimensional model for the simulation of shelf sea dynamics. Deutsche Hydrographische Zeitschrift 38, 165–187.

Beier, E., 1997. A numerical investigation of the annual variability in the Gulf of California. Journal of Physical Oceanography 27, 615–632.

Beier, E., Ripa, P., 1999. Seasonal gyres in the northern Gulf of California. Journal of Physical Oceanography 29, 302–311.

Bernardi, G., Lape, J., 2005. Tempo and mode of speciation in the Baja California disjunct fish species *Anisotremus davidsonii*. Molecular Ecology 14, 4085–4096.

Bradbury, I.R., Snelgrove, P.V.R., 2001. Contrasting larval transport in demersal fish and benthic invertebrates: the roles of behavior and advective processes in determining spatial pattern. Canadian Journal of Fisheries and Aquatic Sciences 58, 811–823.

Carbajal, N. Modeling of the circulation in the Gulf of California, 1993. Ph. D. thesis, Institute fur Meereskunde, Hamburg, 186 pp.

Carrillo-Bribiezca, L.E., Lavín, M.F., Palacios-Hernández, E., 2002. Seasonal evolution of the geostrophic circulation in the northern Gulf of California. Estuarine, Coastal and Shelf Science 54, 157–173.

Carvajal, M.A., Ezcurra, E., Robles, A., 2004. The Gulf of California: natural resource concerns and the pursuit of a vision. In: Glover, L.K., Earl, S.A. (Eds.), Defying Ocean's End: An Agenda for Action. Island Press. 282 pp.

Condie, S.A., Waring, J., Mansbridge, J.V., Cahill, M.L., 2005. Marine connectivity patterns around the Australian continent. Environmental Modelling & Software 20, 1149–1157.

Cudney-Bueno, R., 2007. Marine Reserves, Community-Based Management, and Small-Scale Benthic Fisheries in the Gulf of

California, Mexico. Ph. D. Dissertation, University of Arizona, Tucson, Arizona, 322 pp.

Gutiérrez, O.Q., Marinone, S.G., Parés-Sierra, A., 2004. Lagrangian surface circulation in the Gulf of California from a 3D numerical model. Deep-Sea Research II 51/6-9, 659–672.

Hill, A.E., 1994. Horizontal zooplankton dispersal by diel vertical migration in S2 tidal currents on the northwest European continental shelf. Continental Shelf Research 14, 491–506.

Hofmann, E.E., Haskell, A.G.E., Klinck, J.M., Lacara, C.M., 2004. Lagrangian modeling studies of Antarctic krill (*Euphausia superba*) swarm formation. ICES Journal of Marine Science 61, 617–631.

Hogan, J.D., Mora, C., 2005. Experimental analysis of the contribution of swimming and drifting to the displacement of reef fish larvae. Marine Biology 147, 1213–1220.

James, M.K., Armsworth, P.R., Mason, L.B., Bode, L., 2002. The structure of reef fish metapopulations: modeling larval dispersal and retention patterns. Proceedings of the Royal Society of London. Series B 269, 2079–2086.

Kochergin, V.P., 1987. Three-dimensional prognostic models. In: Heaps, N.S. (Ed.), Three-Dimensional Coastal Ocean Models. American Geophysical Union, Washington, D.C.

Largier, J.L., 2003. Considerations in estimating larval dispersal distances from oceanographic data. Ecological Applications 13, 71–89.

Lavín, M.F. and Marinone, S.G., 2003. An overview of the physical oceanography of the Central Gulf of California. 173-204, 2003. en "O. U. Velasco Fuentes, J. Sheinbaum and J. L. Ochoa de la Torre (Editors), *Nonlinear Processes in Geophysical Fluid Dynamics*. Kluwer Academic Publishers, Dordrecht, The Netherlands. ISBN 1-4020-1589-5. 9654.

Lavín, M.F., Durazo, R., Palacios, E., Argote, M.L., Carrillo, L., 1997. Lagrangian observations of the circulation in the northern Gulf of California. Journal of Physical Oceanography 27, 2298–2305.

Marinone, S.G., 2003. A three dimensional model of the mean and seasonal circulation of the Gulf of California. Journal of Geophysical Research 108 (C10), 3325. doi:10.1029/2002JC001720.

Marinone, S.G., 2006. A numerical simulation of the two- and three-dimensional Lagrangian circulation in the northern Gulf of California. Accepted Estuarine, Coastal and Shelf Science 68, 93–100.

Marinone, S.G., Lavín, M.F., 2005. Tidal current ellipses in a 3D baroclinic numerical model of the Gulf of California. Estuarine, Coastal and Shelf Science 64, 519–530.

Mateos, E., Marinone, S.G., Lavín, M.F., 2006. Role of tides and mixing in the formation of an anticyclonic gyre in San Pedro Mártir Basin, Gulf of California. Deep Sea Res. II 53, 60–76.

Palacios-Hernández, E., Beier, E., Lavín, M.F., Ripa, P., 2002. The effect of the seasonal variation of stratification on the circulation on the northern Gulf of California. Journal of Physical Oceanography 32, 705–728.

Proehl, J.A., Lynch, D.R., McGillicuddy, D.J., Ledwell, J.R., 2005. Modeling turbulent dispersion on the North Flank of Georges Bank using Lagrangian particle methods. Continental Shelf Research 25, 875–900.

Visser, A.W., 1997. Using random walk models to simulate the vertical distribution of particles in a turbulent water column. Marine Ecology Progress Series 158, 275–281.

Wolanski, E., Doherty, P., Carleton, J., 1997. Directional swimming of fish larvae determines connectivity of fish populations on the Great Barrier Reef. Naturwissenschaften 84, 262–268.